







Article

Chemical Profile of *Ruta graveolens*, Evaluation of the Antioxidant and Antibacterial Potential of Its Essential Oil, and Molecular Docking Simulations

Călin Jianu ¹, Ionuț Goleț ², Daniela Stoin ¹, Ileana Cocan ¹, Gabriel Bujancă ¹, Corina Mișcă ^{1,*}, Marius Mioc ^{3,4}, Alexandra Mioc ^{3,4}, Codruța Șoica ^{3,4}, Alexandra Teodora Lukinich-Gruia ^{5,*}, Laura-Cristina Rusu ^{6,7}, Delia Muntean ^{8,9} and Delia Ioana Horhat ⁸

- ¹ Faculty of Food Engineering, Banat's University of Agricultural Sciences and Veterinary Medicine "King Michael I of Romania", 300645 Timișoara, Romania; calin.jianu@gmail.com (C.J.); danielastoin@usab-tm.ro (D.S.); ileanacocan@usab-tm.ro (I.C.); gabrielbujanca@usab-tm.ro (G.B.)
- ² Faculty of Economics and Business Administration, West University of Timișoara, 300233 Timișoara, Romania; ionut.golet@e-uvt.ro
- ³ Faculty of Pharmacy, "Victor Babeș" University of Medicine and Pharmacy, 300041 Timișoara, Romania; marius.mioc@umft.ro (M.M.); alexandra.mioc@umft.ro (A.M.); codrutasoica@umft.ro (C.Ș.)
- ⁴ Research Center for Pharmacotoxicological Evaluations, Faculty of Pharmacy, "Victor Babeș" University of Medicine and Pharmacy, 300041 Timișoara, Romania
- ⁵ OncoGen Centre, County Hospital "Pius Branzu", 300736 Timișoara, Romania
- ⁶ Faculty of Dental Medicine, "Victor Babeș" University of Medicine and Pharmacy, 300041 Timișoara, Romania; laura.rusu@umft.ro
- ⁷ Multidisciplinary Center for Research, Evaluation, Diagnosis and Therapies in Oral Medicine, "Victor Babeș" University of Medicine and Pharmacy, 300173 Timișoara, Romania
- ⁸ Faculty of Medicine, "Victor Babeș" University of Medicine and Pharmacy, 300041 Timișoara, Romania; muntean.delia@umft.ro (D.M.); horhat.ioana@umft.ro (D.I.H.)
- ⁹ Multidisciplinary Research Center on Antimicrobial Resistance, "Victor Babeș" University of Medicine and Pharmacy, 300041 Timișoara, Romania
- * Correspondence: corinamisca@usab-tm.ro (C.M.); alexandra.gruia@gmail.com (A.T.L.-G.)



Citation: Jianu, C.; Goleț, I.; Stoin, D.; Cocan, I.; Bujancă, G.; Mișcă, C.; Mioc, M.; Mioc, A.; Șoica, C.; Lukinich-Gruia, A.T.; et al. Chemical Profile of *Ruta graveolens*, Evaluation of the Antioxidant and Antibacterial Potential of Its Essential Oil, and Molecular Docking Simulations. *Appl. Sci.* **2021**, *11*, 11753. <https://doi.org/10.3390/app112411753>

Academic Editor: Antony C. Calokerinos

Received: 10 November 2021
Accepted: 7 December 2021
Published: 10 December 2021

Publisher's Note: MDPI stays neutral with regard to jurisdictional claims in published maps and institutional affiliations.



Copyright: © 2021 by the authors. Licensee MDPI, Basel, Switzerland. This article is an open access article distributed under the terms and conditions of the Creative Commons Attribution (CC BY) license (<https://creativecommons.org/licenses/by/4.0/>).

Abstract: The research aimed to investigate the chemical composition and antioxidant and antibacterial potential of the essential oil (EO) isolated from the aerial parts (flowers, leaves, and stems) of *Ruta graveolens* L., growing in western Romania. *Ruta graveolens* L. essential oil (RGEO) was isolated by steam distillation (0.29% *v/w*), and the content was assessed by gas chromatography-mass spectrometry (GC-MS). Findings revealed that 2-Undecanone (76.19%) and 2-Nonanone (7.83%) followed by 2-Undecanol (1.85%) and 2-Tridecanone (1.42%) are the main detected compounds of the oil. The RGEO exerted broad-spectrum antibacterial and antifungal effects, *S. pyogenes*, *S. aureus*, and *S. mutans* being the most susceptible tested strains. The antioxidant activity of RGEO was assessed by peroxide and thiobarbituric acid value, 1,1-diphenyl-2-picrylhydrazyl radical (DPPH), and β -carotene/linoleic acid bleaching testing. The results indicated moderate radical scavenging and relative antioxidative activity in DPPH and β -carotene bleaching tests. However, between the 8th and 16th days of the incubation period, the inhibition of primary oxidation compounds induced by the RGEO was significantly stronger ($p < 0.001$) than butylated hydroxyanisole (BHA). Molecular docking analysis highlighted that a potential antimicrobial mechanism of the RGEO could be exerted through the inhibition of D-Alanine-d-alanine ligase (DDI) by several RGEO components. Docking analysis also revealed that a high number RGEO components could exert a potential in vitro protein-targeted antioxidant effect through xanthine oxidase and lipoxygenase inhibition. Consequently, RGEO could be a new natural source of antiseptics and antioxidants, representing an option for the use of synthetic additives in the food and pharmaceutical industry.

Keywords: *Ruta graveolens* L.; essential oil; 2-undecanone; 2-nonanone; antimicrobial activity; antioxidant activity; molecular docking

1. Introduction

Food spoilage may be caused by physical, chemical, or microbiological mechanisms. Microbial spoilage is frequently due to spoilage bacteria, yeasts, or moulds' growth and/or metabolism [1,2]. The chemical spoilage typically occurs when food exposure to oxygen triggers a chain of several chemical reactions involving lipids, fatty acids, and pigments and generates chemical compounds with undesirable biochemical properties, such as toxicity and unpleasant smell, taste, and colour [3]. These changes make foodstuff unacceptable or undesirable for consumption and, finally, generate food loss and waste [2]. The real economic losses generated by food spoilage are challenging to estimate. However, these losses represent a substantial financial burden assessed at 1.3 billion tonnes per year by FAO [4].

Consequently, to increase foodstuff quality, safety, and shelf-life without any adverse effect on their nutritional or sensorial properties, food additives such as preservatives and antioxidants have become indispensable for the food industry, mainly synthetic ones. In recent decades, there has been significant scientific progress concerning pharmacological studies of aromatic plants to identify and valorise natural extracts [5,6]. This trend is concurrent with an increasing interest in identifying new sources of preservatives and antioxidants to replace synthetic food additives because of their potential carcinogenicity [7,8]. A large plethora of plant extracts are also well known and researched for their antimicrobial potential. These extracts contain various compound classes such as terpenes, polyphenolic compounds, flavonoids, various aldehydes, and ketones or alkaloids that disrupt bacteria activity by various mechanisms [9]. These mechanisms include key enzymes that play important roles in bacterial survival and proliferation and are frequently used as targets for novel antimicrobial drug design or for the determination of active antimicrobial agents' mechanisms of action using computational methods [10]; *Rutaceae* family have been recognized for their economic value and also for the cultivated citrus fruits, timber, and essential oils (EOs), indicating a potential source of natural active principles [11–13]. One of the genera of *Rutaceae* family plants investigated is the genus *Ruta* [13]. The genus *Ruta* includes about 40 species of perennial shrubs and herbs distributed along the Mediterranean coast, the Balkan Peninsula, and Crimea [14]. In Romania, the *Ruta* genus is represented by *Ruta graveolens* L., *Ruta suaveolens* D.C., and *Dictamnus albus* L. [15]. Among the family members, *R. graveolens* L. stands out for EO production [6]. Several studies report that oxygenated compounds (e.g., aldehydes, alcohols, and esters) are predominant in the *R. graveolens* EOs (RGEO) isolated from leaves, fruits, flowers, stems, and roots [16]. In contrast, other investigations mention aliphatic compounds, especially ketones (2-undecanone and 2-nonanone), representing more than 50% of the total composition of RGEO [6,14,17]. These differences in the phytochemical profile of *R. graveolens* may explain the anti-rheumatic, anti-diarrheic, anti-inflammatory, anti-febrile, anti-ulcer, anti-diabetics, and antimicrobial properties reported in the recent pharmacological trials [6,18,19]. To our knowledge, no investigation of the antioxidant properties of *R. graveolens* has been previously reported. However, several studies report the in vitro antioxidant properties of the *Ruta montana* and *Ruta chalepensis*. Still, no investigations report the *Ruta* genus members' antioxidant activity in food systems.

This research aimed to investigate: (i) the chemical composition of the EO isolated from the aerial parts of *R. graveolens* cultivated in western Romania by using the GC-MS technique; (ii) the antioxidant and antimicrobial activities of the oil; and (iii) the mechanisms of interaction between RGEO chemical components and target proteins correlated with antibacterial activity and intracellular antioxidant mechanisms, thus aiming for its potential application in food and pharmaceutical industries as a green preservative and/or antioxidant.

2. Materials and Methods

2.1. Plant Material and RGEO Isolation Procedure

The fresh plant material was harvested manually, during the flowering phase in July 2019, from the experimental fields of the Didactic Station "Tinerii Naturaliști"/Banat's

University of Agricultural Sciences and Veterinary Medicine “King Michael I of Romania” in Timisoara, Romania. After identification, a voucher specimen (VSNH.BUASTM-109/1) was deposited in the Herbarium of Agricultural Technologies Department, Faculty of Agriculture, Banat’s University of Agricultural Sciences and Veterinary Medicine “King Michael I of Romania” from Timisoara, Romania. The fresh plant material (flowers, leaves, and stems) was manually chopped into parts approximately 1.5 cm long and immediately submitted to steam distillation [20] in a Craveiro apparatus for 4 h. A water-cooled EO receiver was used to reduce the formation of artifacts due to overheating, which may occur during the isolation of RGEO. After separating the RGEO by decantation (yielding at 0.29% *v/w*), the oil was dried using anhydrous sodium sulphate and stored until use at $-18\text{ }^{\circ}\text{C}$.

2.2. Gas Chromatography Coupled to Mass Spectrometry Method

The RGEO was analyzed using a sensitive and qualitative gas chromatographic technique performed on an HP6890 gas chromatograph coupled with an HP5973 mass spectrometer. The sample, diluted 1:1000 in hexane, was injected in a splitless mode in a heated inlet at $230\text{ }^{\circ}\text{C}$, and run through a Bruker Br-5MS column ($30\text{ m} \times 0.25\text{ mm}$; film thickness $0.25\text{ }\mu\text{m}$) (Agilent Technologies, Santa Clara, CA, USA), carrier gas: helium, flow rate 1.0 mL/min . The gas chromatograph oven temperature was set up to $50\text{ }^{\circ}\text{C}$ for 5 min, raised to $300\text{ }^{\circ}\text{C}$ at a temperature rate of $6\text{ }^{\circ}\text{C/min}$, and kept there for 5 min. The HP5973 mass spectrometer operating parameters were as follows: ionization potential, 70 eV; mass analyzer quadrupole $150\text{ }^{\circ}\text{C}$; solvent delay 3.0 min; mass range 50 to 550 amu. The NIST0.2 spectral library (USA National Institute of Science and Technology software) was employed to identify the compounds (similarity indexes $> 90\%$), followed by a comparison of the retention index (RI), calculated based on the *n*-alkanes $\text{C}_8\text{--C}_{20}$ homologous series, with the values reported in the literature [21].

2.3. Effect of RGEO on Cold-Pressed Sunflowers Oil Oxidation

RGEO and synthetic antioxidants, butylated hydroxyanisole (BHA) and butylated hydroxytoluene (BHT), used for comparison were added at 200 mg/L concentrations separately to 10 mL of cold-pressed sunflower oil purchased from the local market. Oxidation was periodically evaluated by measuring peroxide value (PV) at the 0th, 4th, 8th, 12th, 16th, 20th, and 24th days of storage according to the potentiometric end-point determination method described by ISO 27107:2010 [22]. In addition, the thiobarbituric acid (TBA) value was analysed to measure secondary oxidation products in the cold-pressed sunflower oil at the same days of storage, according to the previous investigation described by Jianu et al. [23]. A negative control sample was prepared under the same conditions without adding any additives. All analyses were performed in triplicate.

2.4. 1,1-Diphenyl-2-picrylhydrazyl Radical (DPPH) Free Radical Scavenging Activity

The radical-scavenging activity of the RGEO with DPPH was established on the scavenging capacity of the stable DPPH· free radical following the Brand-Williams method [24]. Shortly, all samples, RGEO and reference positive controls (δ -tocopherol, BHA, BHT) were diluted in methanol to obtain concentrations between 1.5 and 0.093 mg/mL . Samples were pipetted in triplicate into plates with 96 wells and left to incubate at room temperature in the dark for 30 min. Their absorbances were read at 515 nm against methanol as a negative control at a Tecan i-control 1.10.4.0 Infinite 200Pro spectrophotometer. The obtained results were expressed as a DPPH free radical percentage (I%) and calculated based on the equation: $I\% = (A_{\text{methanol}} - A_{\text{sample}} / A_{\text{methanol}}) \times 100$; A_{methanol} is methanol absorbance, and A_{sample} is the tested sample absorbance. IC_{50} index was calculated with the software BioDataFit 1.02 (Chang Bioscience Inc., Fremont, CA, USA).

2.5. β -Carotene Bleaching Test

The experiment measured the coupled autoxidation of β -carotene and linoleic acid as previously described by Jianu et al. [23]. Briefly, β -carotene (0.5 mg) was added to chloro-

form (1 mL), linoleic acid (25 μ L), and Tween 40 (200 mg). The mixture was evaporated at 45 °C for 5 min under vacuum to remove chloroform. The residue was diluted slowly with distilled water saturated with oxygen (100 mL) and vigorously shaken to form an emulsion. The emulsion (2.5 mL) was transferred to the test tubes containing 350 μ L of RGEO methanolic solution (2 g/L concentration). BHT in methanol was used as a positive control. The test tubes were gently shaken and incubated for 48 h (room temperature) before their absorbances readings at 490 nm. All experiments were performed in triplicate.

2.6. Determination of Antimicrobial Activity

2.6.1. Bacterial Strains

For determining the RGEO antimicrobial activity, the following microbial reference strains were used: Gram-positive cocci (*Enterococcus faecalis* ATCC 51299, *Staphylococcus aureus* ATCC 25923, *Streptococcus pyogenes* ATCC 19615, and *Streptococcus mutans* ATCC 35668), Gram-negative bacilli (*Escherichia coli* ATCC 25922, *Klebsiella pneumoniae* ATCC 700603, *Salmonella enterica* serotype *Typhimurium* ATCC 14028, *Shigella flexneri* serotype 2b ATCC 12022, and *Pseudomonas aeruginosa* ATCC 27853), and two strains of *Candida* species (*Candida albicans* ATCC 10231 and *Candida parapsilosis* ATCC 22019). The methods used to test RGEO antimicrobial activity were performed according to the European Committee on Antimicrobial Susceptibility Testing (EUCAST) [25] and with minimal adjustments based on our previous studies [20,23,26].

2.6.2. Antimicrobial Screening

The disk diffusion method was used for the initial testing of RGEO antimicrobial activity. The microbial suspension was prepared to 0.5 McFarland using a standard saline solution for each strain and inoculated on Mueller-Hinton agar (bioMérieux, Marcy-l'Étoile, France). Afterward, on these plates, a disk (BioMaxima, Lublin, Poland) containing 10 μ L of RGEO to be tested and disks containing 5 μ g levofloxacin and 25 μ g fluconazole for positive control were placed on the surface. The inhibition zones were measured in millimeters after a 24-hour incubation at 35–37 °C for bacteria species and at 28 °C for *Candida* species.

2.6.3. Minimum Inhibitory Concentration

Using the serial dilution method, the microbial suspension was adjusted to 5×10^5 CFU/mL (colony forming units). Serial dilutions of RGEO in DMSO were prepared, ranging from 400 to 12.5 mg/mL concentrations. The following: 0.5 mL microbial suspension, 0.1 mL of each RGEO dilution, and 0.4 mL Mueller Hinton broth, were transferred in six test tubes, obtaining a final inoculum of 0.5×10^5 CFU/mL and a final RGEO dilution from 40 to 1.25 mg/mL. After 24 h of incubation at 37 and at 30 °C, respectively, the test tube containing the lowest RGEO concentration, and no visible growth was considered MIC interpretation.

2.6.4. Minimum Bactericidal Concentration and Minimum Fungicidal Concentration

From the tubes with MIC, 1 μ L was inoculated on Columbia agar and 5% sheep blood for bacterial strains and Sabouraud for *Candida* strains (bioMérieux, Marcy-l'Étoile, France). The inoculated plates were incubated for appropriately 24 h, and the lowest concentration with no visible growth was considered for MBC or MFC.

2.7. In Silico Molecular Docking

Molecular docking analysis was achieved using a previously described method [27]. All protein target structures were retrieved from the RCSB Protein Data Bank [28] (Table 1). These structures were optimized as suitable docking targets, using Autodock Tools v1.5.6 (The Scripps Research Institute, La Jolla, CA, USA). The protein structure file was prepared by removing water molecules, unlinked atoms/protein chains, and the native ligands after which the potential of the protein target was assigned with Kollman charges, a feature imbedded in the software. The target structures were saved as pdbqt files. The structures

of the 37 RGEO compounds were generated based on their available SMILE strings (or isomeric SMILE strings in case of enantiomers), using BIOVIA Draw (Dassault Systems BIOVIA). The 2D structures were converted into 3D structures using PyRx's Open Babel module by using 500 steps of a steepest descent geometry optimization with the MMFF94 forcefield. The lowest energy conformer generation does not alter the stereochemistry of the input structures. Molecular docking was achieved with the PyRx v0.8 virtual screening software (The Scripps Research Institute, La Jolla, CA, USA) using Vina's encoded scoring function [29]. This is a custom scoring function which combines, as their developers describe, empirical information from both the conformational preferences of the receptor-ligand complexes and experimental affinity measurements [29]. The docking software was set to generate/dock 10 conformers of each input molecular structure. The docking protocol was validated by re-docking the native ligands into their original protein binding sites. The root means square deviation (RMSD) between the predicted and experimental docking pose of the native ligand was calculated. Molecular docking was performed only for cases with aforementioned RMSD values not exceeding a 2 Å threshold. The docking grid box coordinates and size were selected to best fit the active binding site (Table 1). Docking scores were recorded as ΔG binding energy values (kcal/mol). Protein-ligand binding interactions were analysed using Accelrys Discovery Studio 4.1 (Dassault Systems BIOVIA, San Diego, CA, USA).

Table 1. Molecular docking parameters for each protein target.

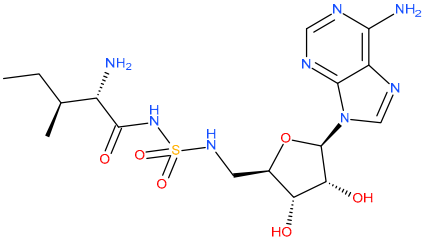
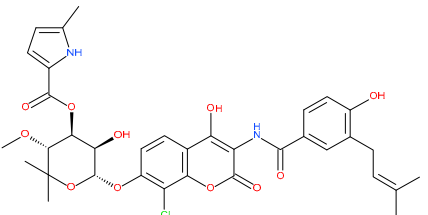
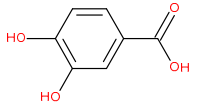
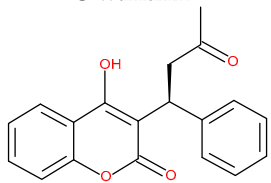
Protein	PDB ID/ Protein Structure Resolution	Grid Box Center Coordinates	Grid Box Size	Native Ligand	References
IARS	1JZQ 3.00 Å	center_x = -27.683 center_y = 7.940 center_z = -28.726	size_x = 15.314 size_y = 10.229 size_z = 10.025	N-[isoleuciny]-n'-[adenosyl]-diaminosufone 	[30]
DNA gyrase	1KZN 2.30 Å	center_x = 17.221 center_y = 31.155 center_z = 36.750	size_x = 11.994 size_y = 13.471 size_z = 14.454	Clorobiocin 	[31]
Lipoxygenase	1N8Q 2.10 Å	center_x = 21.088 center_y = 1.163 center_z = 19.056	size_x = 10.291 size_y = 6.561 size_z = 8.855	Protocatechuic acid 	[32]
CYP2C9	1OG5 2.55 Å	center_x = -19.429 center_y = 87.688 center_z = 39.060	size_x = 10.873 size_y = 15.624 size_z = 9.745	S-warfarin 	[33]

Table 1. Cont.

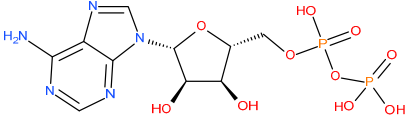
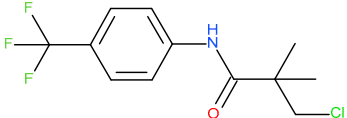
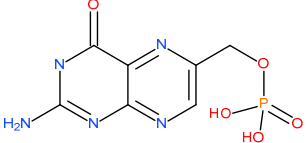
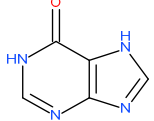
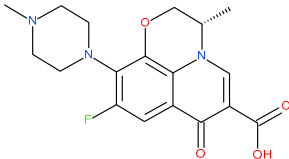
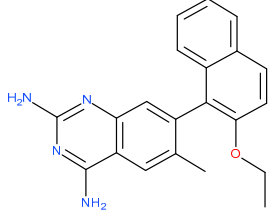
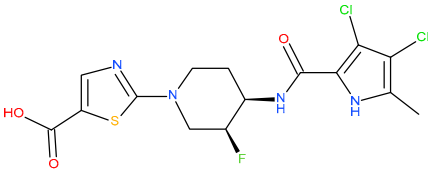
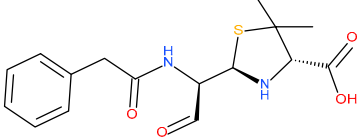
Protein	PDB ID/ Protein Structure Resolution	Grid Box Center Coordinates	Grid Box Size	Native Ligand	References
NADPH-oxidase	2CDU 1.80 Å	center_x = 18.043 center_y = -6.494 center_z = 0.261	size_x = 13.845 size_y = 13.580 size_z = 19.019	ADP 	[34]
DDI1	2I80 2.19 Å	center_x = 34.136 center_y = 4.049 center_z = 25.365	size_x = 8.407 size_y = 10.984 size_z = 10.984	3-chloro-2,2-dimethyl-N-[4-(trifluoromethyl)phenyl]propanamide 	[35]
DHPS	2VEG 2.40 Å	center_x = 29.308 center_y = 47.975 center_z = -0.104	size_x = 11.994 size_y = 10.138 size_z = 8.233	Pterin-6-yl-methyl-monophosphate 	[36]
Xanthine oxidase	3NRZ 1.80 Å	center_x = 37.638 center_y = 19.857 center_z = 17.684	size_x = 6.767 size_y = 10.461 size_z = 8.873	Hypoxanthine 	[37]
Type IV topoisomerase	3RAE 2.90 Å	center_x = -33.590 center_y = 67.448 center_z = -25.612	size_x = 14.217 size_y = 9.518 size_z = 6.868	Levofloxacin 	[38]

Table 1. Cont.

Protein	PDB ID/ Protein Structure Resolution	Grid Box Center Coordinates	Grid Box Size	Native Ligand	References
DHFR	3SRW 1.70 Å	center_x = −4.932 center_y = −31.078 center_z = 6.811	size_x = 11.512 size_y = 12.532 size_z = 9.986	7-(2-ethoxynaphthalen-1-yl)-6-methylquinazoline-2,4-diamine 	[39]
DNA gyrase subunit B	3TTZ 1.63 Å	center_x = 16.304 center_y = −18.973 center_z = 5.866	size_x = 18.223 size_y = 11.865 size_z = 9.461	2-[(3S,4R)-4-[[[(3,4-dichloro-5-methyl-1H-pyrrol-2-yl)carbonyl]amino]-3-fluoropiperidin-1-yl]-1,3-thiazole-5-carboxylic acid 	[40]
PBP1a	3UDI 2.60 Å	center_x = 33.807 center_y = −0.788 center_z = 12.228	size_x = 10.343 size_y = 8.297 size_z = 10.636	Penicillin G-open form 	[41]

2.8. Statistical Analysis

The main approach for statistical testing the antioxidant property of RGEO was the ANOVA method, with samples (synthetic antioxidants and RGEO) and incubation period as main effects, followed by a post-hoc analysis. The overall ANOVA analysis shows that the main effects and interaction effects are highly significant ($p < 0.001$) for PV and TBA values. Because the number of observations of each sample per incubation period is low (nine values), the normality assumption was tested on the ANOVA residuals using the Shapiro–Wilk test. The null hypothesis was not rejected in the case of PV ($p = 0.182$) but was rejected in the case of TBA ($p < 0.001$). Consequently, the post-hoc analysis was performed using the Tukey parametric test in the case of PVs. Instead, the post-hoc analysis was performed using Dun’s non-parametric test with Bonferroni correction for the TBA values. To take into account the interaction effect, all the pairwise comparisons were performed separately, for each incubation period at a time; also worth mentioning is that the groups have homogenous variances at this level of analysis according to Leven’s test. In the case of the scavenging effect on the DPPH radical assay, we faced the situation of non-normality (Shapiro–Wilk, $p = 0.005$) of ANOVA residuals, non-homogeneity of variances across groups (Levene, $p < 0.001$), and a low number of observations per group (nine measurements). Therefore, the data have been normalized by using the natural logarithm transformation. In addition, the Games-Howell test was used in post-hoc analysis to address the lack of variance homogeneity. Finally, the ANOVA approach followed by Tukey’s test in the post-hoc analysis was applied to assess the antimicrobial properties. The ANOVA residuals have close to normality distribution (Shapiro–Wilk, $p = 0.844$), and the groups (three inhibition zone measurements per group) are homogenous from a variance point of view (Levens’s, $p = 0.28$). Data analysis was completed using JASP (Version 0.15), and p -values < 0.05 were considered as significant.

3. Results

3.1. Chemical Composition of RGEO

Steam distillation of the fresh plant material of *R. graveolens* gave a yellowish oil with an intense and penetrating odour with a yield of 0.29% (v/w). The extraction yields obtained for *R. graveolens* are comparable to those reported in the literature [17,42–45]. As previously reported by Formisano et al. [46], the total EO content of plants was affected by genetic background, environmental conditions, and soil composition.

GC-MS analysis of the RGEO identifies thirty-seven compounds (Figure 1 and Table 2), representing 98.68% of the obtained oil. The main detected compounds are 2-Undecanone and 2-Nonanone at 76.19% and 7.83%, respectively, followed by 2-Undecanol at 1.85% and 2-Tridecanone at 1.42%. The abundance of 2-Undecanone in RGEO is in accord with the previous studies conducted on RGEOs from Egypt [47], Algeria [45], Iran [48], and Saudi Arabia [49]. However, the proportions and nature of the identified chemical compounds of the analysed EOs are not always the same compared with the previous studies. These differences may be due to genetic, distinct environmental and climatic conditions, geographic origins, and plant populations [49,50].

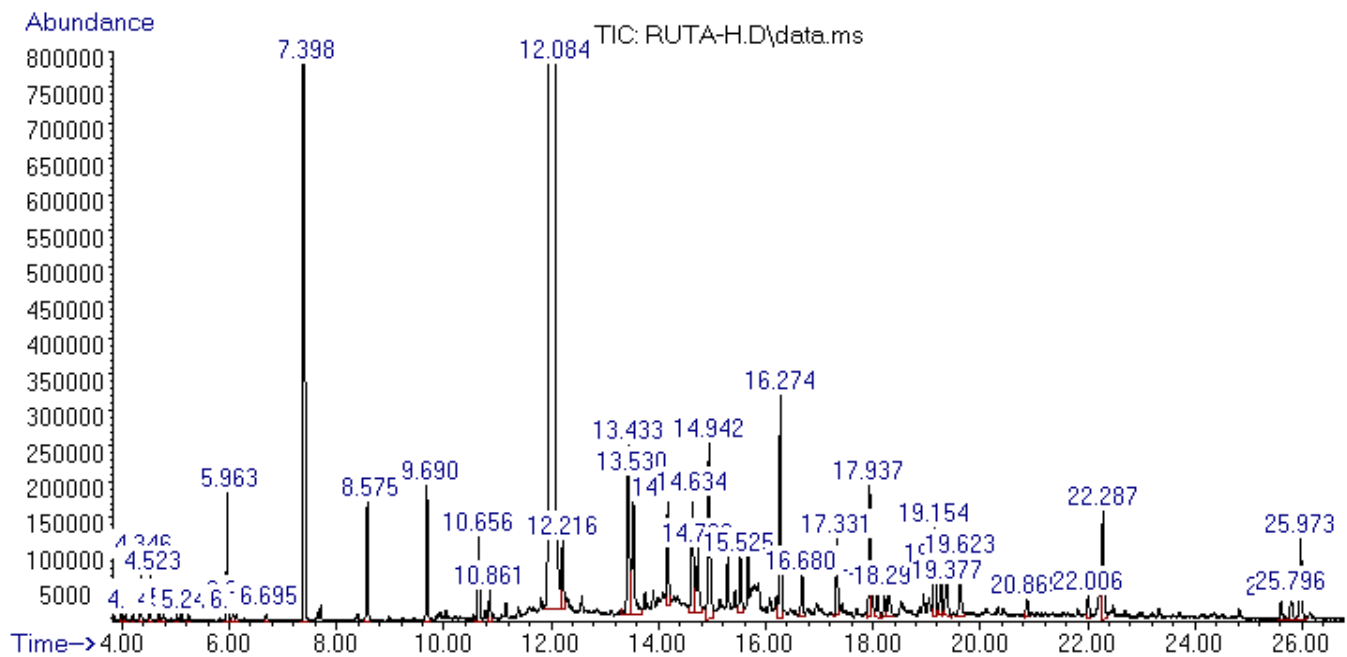


Figure 1. Gas chromatogram of RGE0 cultivated in western Romania.

Table 2. Chemical composition of RGE0 cultivated in western Romania.

No	Compounds	KI ^a	%
1.	3-Octanone	908	0.06
2.	beta-Thujene	912	tr.
3.	4-Carene, (1S,3S,6R)-(-)	919	tr.
4.	Hydroperoxide, 1-ethylbutyl	925	0.24
5.	Hydroperoxide, 1-methylpentyl	934	0.19
6.	(2E)-2-Hexenyl benzoate	942	tr.
7.	1-Cyclohexyl-2-propen-1-ol	947	tr.
8.	2-Bornene	959	tr.
9.	para-Cymene	1005	0.58
10.	beta-Terpinyl acetate	1011	0.08
11.	Eucalyptol	1014	tr.
12.	4-Carene, (1S,3R,6R)-(-)	1042	0.06
13.	2-Nonanone	1076	7.83
14.	2-Decanone	1190	0.75
15.	Cyclopropanecarboxylic acid, nonyl ester	1238	0.49
16.	(S)-(+)-Carvone	1248	0.18
17.	2-Undecanone	1308	76.19
18.	2-Undecanol	1315	1.85
19.	1-methyl-cycloundecanol	1380	1.13
20.	2-Dodecanone	1412	0.63
21.	beta-Caryophyllene	1439	0.55
22.	2-Acetoxytetradecane	1450	1.34
23.	Germacrene-D	1478	0.42
24.	2-Tridecanone	1515	1.42
25.	Hexa-hydro-farnesol	1536	0.28
26.	Elemol	1568	0.48
27.	9-Methyl-10-methylenetricyclo [4.2.1.1(2,5)]decan-9-ol	1598	0.81
28.	2,5-Octadecadiynoic acid, methyl ester	1605	0.19
29.	4-(3,4-Methylenedioxyphenyl)-2-butanone	1612	0.15
30.	Ascaridole epoxide	1615	0.24
31.	Valeric acid, 2-tridecyl ester	1658	0.59

Table 2. Cont.

No	Compounds	KI ^a	%
32.	Geranyl isovalerate	1663	0.32
33.	alpha-Eudesmol	1669	0.38
34.	1,2,3,3a,4,9,10,10a-Octahydrobenzo[f]azulene	1681	0.40
35.	Corymbolone	1743	0.13
36.	Methoxsalen	1977	0.16
37.	Bergaptene	1995	0.56
		Total:	98.68

^a Retention indices (RIs) calculated upon the calibration curve of alkane C₈–C₂₀ standard injected and analyzed in the same conditions as RGEO.; tr. (trace) < 0.05.

3.2. Antioxidant Activity

The formation of primary lipid oxidation products throughout 24 days of storage of the samples was measured using the amount of PV. The effect of RGEO, BHA, and BHT on PV changes in cold-pressed sunflower oil lipids has been shown in Table 3. The PV of samples treated with RGEO, after 8 days and 16 days of incubation, were lower than the values of the control sample and samples treated with BHA and BHT, with a high significance level ($p < 0.001$). After 12 days of incubation, the PV of the sample treated with RGEO was lower than the values of the control sample and sample containing BHA but higher than the values of the sample containing BHT with high significance in all cases ($p < 0.01$). Finally, after 20 days and 24 days of incubation, the PV of the sample treated with RGEO was significantly lower than the control sample values ($p < 0.001$) and significantly higher than the samples treated with BHA and BHT ($p < 0.001$).

Table 3. The antioxidant effects of RGEO, BHA, and BHT in terms of peroxide values (meq of oxygen kg⁻¹).

Storage Time (Days)	PV (meq of Oxygen kg ⁻¹)			
	Control Sample	BHT	BHA	RGEO
0 days	1.97 ± 0.05 ^{bc}	1.88 ± 0.04 ^a	1.93 ± 0.06 ^{ab}	2 ± 0.04 ^c
4 days	3.1 ± 0.06 ^a	2.98 ± 0.06 ^c	3.21 ± 0.06 ^b	3.13 ± 0.09 ^{ab}
8 days	5.67 ± 0.07 ^a	4.28 ± 0.04 ^b	5.9 ± 0.06 ^c	4.01 ± 0.05 ^d
12 days	7.7 ± 0.05 ^a	5.91 ± 0.06 ^b	7.06 ± 0.07 ^c	6.56 ± 0.08 ^d
16 days	9.73 ± 0.07 ^a	8.66 ± 0.08 ^b	8.68 ± 0.04 ^b	8.19 ± 0.05 ^c
20 days	12.12 ± 0.05 ^a	9.58 ± 0.03 ^b	9.82 ± 0.06 ^c	9.95 ± 0.06 ^d
24 days	15.91 ± 0.07 ^a	10.03 ± 0.05 ^b	10.11 ± 0.08 ^b	11.49 ± 0.08 ^c

Values with different superscripts are significantly different ($p < 0.05$) according to Tukey test; each value is the Mean ± SD.

TBA value has been extensively applied to evaluate the degree of lipid oxidation. TBA reactive substances are reckoning the second stage auto-oxidation, during which peroxides are oxidized to aldehyde and ketone [51]. The changes in TBA value of different treatment samples during 24 days are shown in Table 4. Generally, the values of samples treated with RGEO were closer to BHA values in the case of TBA measurements. From day 0 through day 20, the TBA values of samples treated with RGEO were higher than those of samples treated with BHA, but the difference was not significantly different, with only one exception, day 4. However, after 24 days of incubation, the values of TBA were lower for samples treated with RGEO but not significantly different according to Dunn's test ($p = 0.32$). Regarding the TBA values of samples treated with BHT, samples treated with RGEO were significantly higher after 4 through 20 days of incubation.

Table 4. The antioxidant effects of RGEO, BHA, and BHT in terms of thiobarbituric acid value (TBA) ($\mu\text{g malondialdehyde g}^{-1}$).

Storage Time (Days)	TBA ($\mu\text{g Malondialdehyde g}^{-1}$)			
	Control Sample	BHT	BHA	RGEO
0 days	2.62 \pm 0.04 ^a	2.5 \pm 0.12 ^b	2.55 \pm 0.08 ^{ab}	2.56 \pm 0.06 ^{ab}
4 days	3.08 \pm 0.04 ^{ab}	2.85 \pm 0.04 ^c	2.88 \pm 0.05 ^{ac}	4.4 \pm 0.06 ^b
8 days	7.51 \pm 0.07 ^a	3.46 \pm 0.05 ^b	4.55 \pm 0.11 ^{bc}	6.54 \pm 0.11 ^{ac}
12 days	10.97 \pm 0.06 ^a	5.18 \pm 0.08 ^b	6.66 \pm 0.15 ^{bc}	9.49 \pm 0.1 ^{ac}
16 days	15.77 \pm 0.1 ^a	5.9 \pm 0.05 ^b	8.06 \pm 0.07 ^{bc}	10.38 \pm 0.11 ^{ac}
20 days	19.48 \pm 0.2 ^a	6.67 \pm 0.22 ^b	11.43 \pm 0.08 ^{bc}	12.41 \pm 0.16 ^{ac}
24 days	28.93 \pm 0.04 ^a	7.3 \pm 0.13 ^b	14.55 \pm 0.08 ^{ac}	14.35 \pm 0.12 ^{bc}

Values with different superscripts are significantly different ($p < 0.05$) according to Dunn's test; each value is the Mean \pm SD.

Antioxidants interact with 1,1-diphenyl-2-picrylhydrazyl radical, a stable free radical, and transform it into 1,1-diphenyl-2-picrylhydrazine. The degree of discoloration demonstrates the radical scavenging potential or the hydrogen-donating ability of the compounds [52]. RGEO was able to reduce the stable free radical DPPH with an IC_{50} value of 0.25 ± 0.09 mg/mL (Table 5). Even if the effect of the radical scavenging activity of RGEO is comparable to that of the delta-tocopherol (IC_{50} : 0.16 ± 0.02 mg/mL), it is not statistically significant ($p = 0.133$) according to the Games-Howell test. In contrast, BHA (IC_{50} : 0.09 ± 0.01 mg/mL) and BHT (IC_{50} : 0.02 ± 0.02 mg/mL) exhibited significantly ($p < 0.05$) better antioxidant activity than RGEO (Table 5). Recently, Benoli et al. (2020) reported DPPH scavenging abilities for Moroccan oil of *R. montana* with an IC_{50} value of 0.244 mg/mL [53]. In contrast, Mohammedi et al. (2018) found IC_{50} values ranging from 0.0496 to 0.0634 mg/mL for *R. montana* oils collected from different regions in Algeria [54]. Similar results were reported by Jaradat et al. (2017) that found IC_{50} values ranging from 0.0069 to 0.0199 mg/mL for Palestinian *R. chalepensis* volatile oils [55], and by Althaher et al. (2021) that reported an IC_{50} value of 0.035 mg/mL for Jordanian *R. chalepensis* oil [56].

Table 5. Antioxidant activities of the RGEO by DPPH and β -carotene–linoleic acid bleaching test.

Parameter	RGEO	Delta-Tocopherol	BHA	BHT
DPPH, IC_{50} (mg/mL)	0.25 \pm 0.09 ^a	0.16 \pm 0.02 ^a	0.09 \pm 0.01 ^b	0.02 \pm 0.02 ^c
β -carotene bleaching (RAA) (%)	77.42 \pm 0.07	Nd	Nd	100

Values with different superscripts are significantly different ($p < 0.05$) according to Games-Howell test; each value is the Mean \pm SD; Nd—not detected.

The β -Carotene bleaching test is based on the discoloration of β -carotene determined to its reaction with radicals produced by linoleic acid oxidation in an emulsion. The antioxidants' presence can decrease the rate of β -carotene bleaching [57,58]. The relative antioxidant activity percentage (RAA%) of RGEO was calculated with the formula $\text{RAA} = A_{\text{RGEO}}/A_{\text{BHT}}$, where A_{RGEO} is the absorption of RGEO, and A_{BHT} is the absorption of BHT (positive control used). Compared with BHT, *R. graveolens* oil bleached β -carotene by $77.42 \pm 0.07\%$ (Table 5). Similar results were reported by Loizzo et al. (2017) for leaf extracts obtained from *R. chalepensis* [59]. However, no previous research were available in the literature concerning the in vitro and in vivo antioxidant activity of RGEO to support us to compare the results directly.

3.3. Antimicrobial Activity

The in vitro antimicrobial activity of RGEO against nine bacteria and fungal strains was evaluated qualitatively and quantitatively by the presence or absence of inhibition zones, MIC, MBC, and MFC values. The diameters of the inhibition zone of RGEO, which include the diameter (6 mm) of the paper disk against the microorganisms tested, are shown in Table 6. The diameters of the inhibition zone induced by RGEO against the tested microorganism strains ranged between 15.21 ± 0.14 mm and 20.61 ± 0.21 mm, suggesting that the oil exerts low to moderate antimicrobial effects. The results revealed that *S. pyogenes*, *S. aureus*, and *S. mutans* were the most susceptible tested strain to the RGEO action, followed by *C. albicans* > *C. parapsilosis* > *E. faecalis* > *P. aeruginosa* > *E. coli* > *K. pneumoniae* > *S. enterica* > *S. flexneri*. Our results agree with previous studies [6,45,49], which reported that RGEO exhibited antimicrobial activity against *S. aureus*, *E. faecalis*, *E. coli*, *K. pneumoniae*, and *C. albicans*. The recorded MICs, MBCs, and MFCs for the tested strains were 1.25, 2.5, and 5 mg/mL, respectively. According to Aligiannis et al. [60], a strong MIC EOs can hold up to 0.5 mg/mL, moderate for MIC 0.6–1.5 mg/mL, and low for MIC above 1.5 mg/mL. The RGEO exhibited a moderate MIC for *S. mutans* and *S. pyogenes* and showed low activity against the rest of the analyzed bacteria. Overall, RGEO showed low efficiency in inhibiting the Gram-negative strains compared to Gram-positive strains, following previous studies [6,27,49,61,62]. These differences in susceptibility could be associated with different rates of penetration of EO constituents into the cell wall and cell membrane structures. Therefore, the ability of EO to disrupt the permeability barrier of cell membrane structures and the accompanying loss of chemiosmotic control are the most likely reasons for its lethal action [63].

Table 6. Antimicrobial of the RGEO by disk diffusion, minimum inhibitory concentration (MIC), minimum bactericidal concentration (MBC), and minimum fungicidal concentration (MFC).

Bacterial and Yeast Strains	Disk Diffusion (mm)	MIC Value (mg/mL)	MBC Value (mg/mL)	MFC Value (mg/mL)
<i>Streptococcus mutans</i>	19.77 ± 0.26 ^b	1.25	1.25	-
<i>Streptococcus pyogenes</i>	20.61 ± 0.21 ^a	1.25	1.25	-
<i>Staphylococcus aureus</i>	19.89 ± 0.14 ^b	2.5	2.5	-
<i>Enterococcus faecalis</i>	16.56 ± 0.17 ^d	2.5	2.5	-
<i>Escherichia coli</i>	15.76 ± 0.1 ^{fe}	5.0	5.0	-
<i>Klebsiella pneumoniae</i>	15.71 ± 0.13 ^{fe}	5.0	5.0	-
<i>Salmonella enterica</i>	15.65 ± 0.23 ^{fe}	5.0	5.0	-
<i>Shigella flexneri</i>	15.21 ± 0.14 ^f	5.0	5.0	-
<i>Pseudomonas aeruginosa</i>	15.95 ± 0.08 ^{de}	5.0	5.0	-
<i>Candida albicans</i>	18.66 ± 0.26 ^c	2.5	-	2.5
<i>Candida parapsilosis</i>	18.42 ± 0.39 ^c	2.5	-	2.5

Values with different superscript are significantly different ($p < 0.05$) according to Tukey test; each value is the Mean \pm SD.

3.4. In Silico Prediction of Mechanism by Molecular Docking Analysis

Ligand-based molecular docking is a computational technique that can be used, among other methods, as a starting point for understanding the targeted mechanism of action of a given molecular structure. In the form of free-binding energy values, the obtained results may indicate an increased/decreased affinity of the analyzed molecule towards the selected target compared to the native ligand (a known inhibitor), given that the binding energy decreases when the compounds' affinity increases [64–66]. For our current study, we used a molecular docking-based protocol to identify possible protein targets for the 37 RGEO components, whose inhibition could be correlated with their in vitro antimicrobial

activity. The same method was also employed to provide an insight regarding a potential in vitro protein targeted based antioxidant activity, apart from the chemical structure related antioxidant activity described above. Protein targets, usually associated with bactericidal/bacteriostatic effects, such as dihydropteroate synthase (DHPS), dihydrofolate reductase (DHFR), D-alanine: D-alanine ligase (Ddl), penicillin binding protein 1a (PBP1a), DNA gyrase, type IV topoisomerase, and isoleucyl-tRNA synthetase (IARS), were used in the present work [10]. Furthermore, molecular docking screening was also employed to assess the RGEO components inhibitory potential towards protein targets that play active roles in intracellular antioxidant mechanisms. To achieve this goal CYP2C9, lipoxygenase xanthine oxidase, and NADPH-oxidase [67] were selected as protein targets.

Docking scores recorded as ΔG values (kcal/mol) corresponding to the 37 docked compounds and the native ligands of each protein are presented in Table 7. However, we intended to spot a trend related to a possible protein-targeted cumulative mechanism of action associated with the set of 37 RGEO compounds in the sense that if a majority of the RGEO components score better or comparable docking results with the native ligand of a target protein, then that cumulative effect may lead to the observed biological activity. To better visualize this tendency, firstly, the docking scores corresponding to each protein target column were reordered in descending order, the lowest ΔG value representing the highest affinity for that specific target. Subsequently, we generated a heatmap based on the rearranged table. Each table column was colored with a three-color scheme gradient, ranging from red for the ΔG value scored by the native ligand (used as control), through white for the midpoint interval, and to blue for the highest value (the structure with the lowest affinity), respectively. Thus, the columns of the target proteins where most of the compounds obtained good docking scores compared to the native ligands will be colored predominantly red (Figure 2).

Table 7. Docking results (binding energy, ΔG kcal/mol) for RGEO 37 compounds.

	1N8Q	1OG5	2CDU	3NRZ	1JZQ	1KZN	2VEG	3RAE	3SRW	3TTZ	3UDI	2I80
	Free Binding Energy ΔG (kcal/mol)											
NL	−5.8	−9.8	−9.3	−6.7	−8.8	−9.3	−6.9	−4.3	−9.9	−8.5	−7.4	−8.4
1	−4.8	−4.7	−4.7	−5.8	−4.3	−4.4	−4	−2.3	−4.5	−4.7	−3.9	−5.4
2	−5.8	−5.5	−5.2	−4.5	−4.8	−4.7	−3.8	−2.1	−5.7	−4.9	−4.4	−5.8
3	−7.1	−5.6	−5.8	−4.3	−5.2	−5.2	−4	−2.4	−6.2	−5.5	−4.6	−6.3
4	−4.7	−4.2	−4.3	−5.6	−3.9	−4.4	−4.1	−2.6	−4.3	−4.6	−4	−4.9
5	−4.8	−4.3	−4.3	−5.5	−4	−4.5	−4	−2.7	−4.6	−4.8	−4.1	−4.9
6	−5.2	−6.8	−6.3	−6.8	−5.8	−5.6	−5.3	−2.9	−6.2	−6.2	−5.3	−6.9
7	−5.8	−5.6	−5.5	−6.7	−5.1	−5	−4.7	−2.9	−5.7	−5.6	−4.6	−6
8	−3.3	−5.6	−5.7	1.7	−4.6	−4.2	−3.7	−2.1	−5.5	−4.7	−4.5	−6.2
9	−6.1	−6.2	−5.7	−6.9	−5.1	−5.3	−4.4	−2.3	−5.6	−5.8	−4.8	−5.9
10	−3.7	−6.8	−6.2	−6.5	−5.9	−5.7	−5.2	−3.4	−6.3	−6.3	−5.7	−6.8
11	−3.6	−5.6	−6	2.8	−4.8	−4.6	−3.7	−2.6	−5.9	−5	−4.8	−6
12	−7.1	−5.7	−5.8	−4.3	−5.1	−5.2	−4	−2.4	−6.2	−5.5	−4.6	−6.3
13	−4.7	−5	−4.9	−5.9	−4.6	−4.5	−3.7	−2.4	−4.8	−5.1	−3.9	−5.8
14	−4.8	−5.4	−4.8	−6.2	−4.7	−4.6	−4.2	−2.3	−5	−5.4	−4	−5.8
15	−4.3	−5.7	−5.3	−5.5	−4.9	−4.6	−4.8	−2.6	−5.4	−5.3	−4.6	−6.6
16	−5.3	−6.4	−6.2	−7.3	−5.7	−5.5	−4.8	−3.2	−5.9	−6	−5.2	−6.2
17	−4.7	−5.3	−5.2	−6	−4.9	−4.4	−4.1	−2.4	−5	−5.1	−4.2	−6
18	−5.3	−5.4	−5	−5.7	−5	−4.5	−4.3	−2.2	−5.2	−5.1	−4.3	−6.1

Table 7. Cont.

	1N8Q	1OG5	2CDU	3NRZ	1JZQ	1KZN	2VEG	3RAE	3SRW	3TTZ	3UDI	2I80
	Free Binding Energy ΔG (kcal/mol)											
19	−2.5	−6.2	−6.3	−3	−5.8	−5.3	−4.8	−3.4	−7.1	−6.5	−5.5	−3.4
20	−4.8	−5.5	−4.8	−5.7	−4.8	−4.7	−4.5	−2.4	−5.2	−5	−4.2	−6.4
21	−0.5	−7.3	−6.5	0.4	−6.3	−6.1	−4.9	−3	−7.6	−6.5	−6.2	−4.3
22	−2	−5.7	−5.8	−2.8	−5.4	−4.8	−4.2	−2.2	−5.9	−5.7	−5.1	−6.2
23	−1.3	−7.1	−6.5	−1.2	−6.8	−6.4	−5.3	−3	−7.7	−6.6	−6.2	−4.4
24	−4.7	−5.6	−5.1	−5.3	−4.9	−4.7	−4.4	−2.1	−5.4	−5.5	−4.5	−6.4
25	−2.1	−6.4	−6.3	−4.3	−5.7	−5.4	−5.1	−2.7	−6.1	−6.4	−5.6	−6.3
26	−2	−6.7	−6.6	−0.8	−6	−6.1	−4.6	−3	−7	−6.7	−5.9	−6.3
27	−0.4	−6.2	−6.7	2.5	−5.3	−5.1	−4.1	−3.2	−6.6	−5.6	−5.8	−5.3
28	0.7	−6	−5.6	−1.1	−5.1	−5.2	−4.8	−2.4	−6.4	−6	−5.1	−5.4
29	−2.9	−6.4	−6.5	−8	−5.8	−5.7	−5.2	−3.3	−6.6	−6.6	−5.8	−7.1
30	−4.7	−5.9	−6.2	−1.2	−5.9	−5.1	−5.1	−3.8	−6.2	−5.6	−5.9	−5.7
31	0.6	−5.5	−5.3	0.3	−4.8	−4.6	−4.5	−2.4	−5.6	−5.5	−4.9	−5.9
32	−2.3	−6.4	−5.8	−3.6	−5.6	−5.5	−5	−2.9	−6.3	−5.9	−5.8	−6.1
33	−2.7	−7.2	−7.2	−2.3	−6.7	−7.6	−5.4	−3.3	−7.8	−7	−6.6	−6.4
34	−0.8	−8.5	−7	−6.7	−7	−6.9	−5.7	−3.1	−7.7	−7.3	−6	−5.7
35	2.9	−7	−6.2	6.1	−6.2	−5.7	−4.6	−3.6	−7.8	−6	−5.4	−2.9
36	−3.7	−7	−7.4	−6.5	−6.8	−6.7	−6.4	−4.3	−7.3	−7.2	−7	−5.4
37	−3.7	−7.1	−7.1	−6.2	−6.3	−6.9	−6.2	−4.3	−7.4	−7.2	−6.4	−6.2

NL—native ligand; highlighted values represent cases where ΔG values of the respective compounds are lower than ΔG of the NL.

Concerning the set of proteins related to RGEO's antibacterial activity, our results show an increased affinity of the majority of docked molecules towards the DDI protein (2I80). DDI is an essential key enzyme involved in bacterial wall biosynthesis and an important drug target for developing new antibiotic agents. This enzyme is responsible for the formation of the dipeptide D-alanine: D-alanine, in a two-step reaction, sequentially by using D-alanine and ATP as substrates for the first reaction step and another D-alanine to complete the reaction [35]. The analyzed compounds were docked in an allosteric pocket adjacent to the D-Ala and ATP binding site. Of the docked compounds, various structures showed a good affinity towards DDI compared to the native ligand, in the range of 2.1 kcal/mol. These structures include monoterpenoids (β -Terpinyl acetate, −6.8 kcal/mol; 4-Carene, −6.3 kcal/mol), sesquiterpenes (Hexa-hydro-farnesol, −6.3 kcal/mol; Elemol −6.3 kcal/mol, α -Eudesmol, −6.4 kcal/mol), esters (Cyclopropanecarboxylic acid, nonyl ester, −6.6 kcal/mol; (2E)-2-Hexenyl benzoate, −6.9 kcal/mol), and ketones (2-Tridecanone, −6.4 kcal/mol; 4-(3,4-Methylenedioxyphenyl)-2-butanone, −7.1 kcal/mol). These findings can be correlated with previous studies that have clearly shown that monoterpenes or terpene-rich EOs are bactericidal and induce bacterial wall disruption, causing the loss of essential nutrients [68,69]. Additionally, based on the present computational data, the antibacterial effect of RGEO may be attributed more to the lower occurring components.

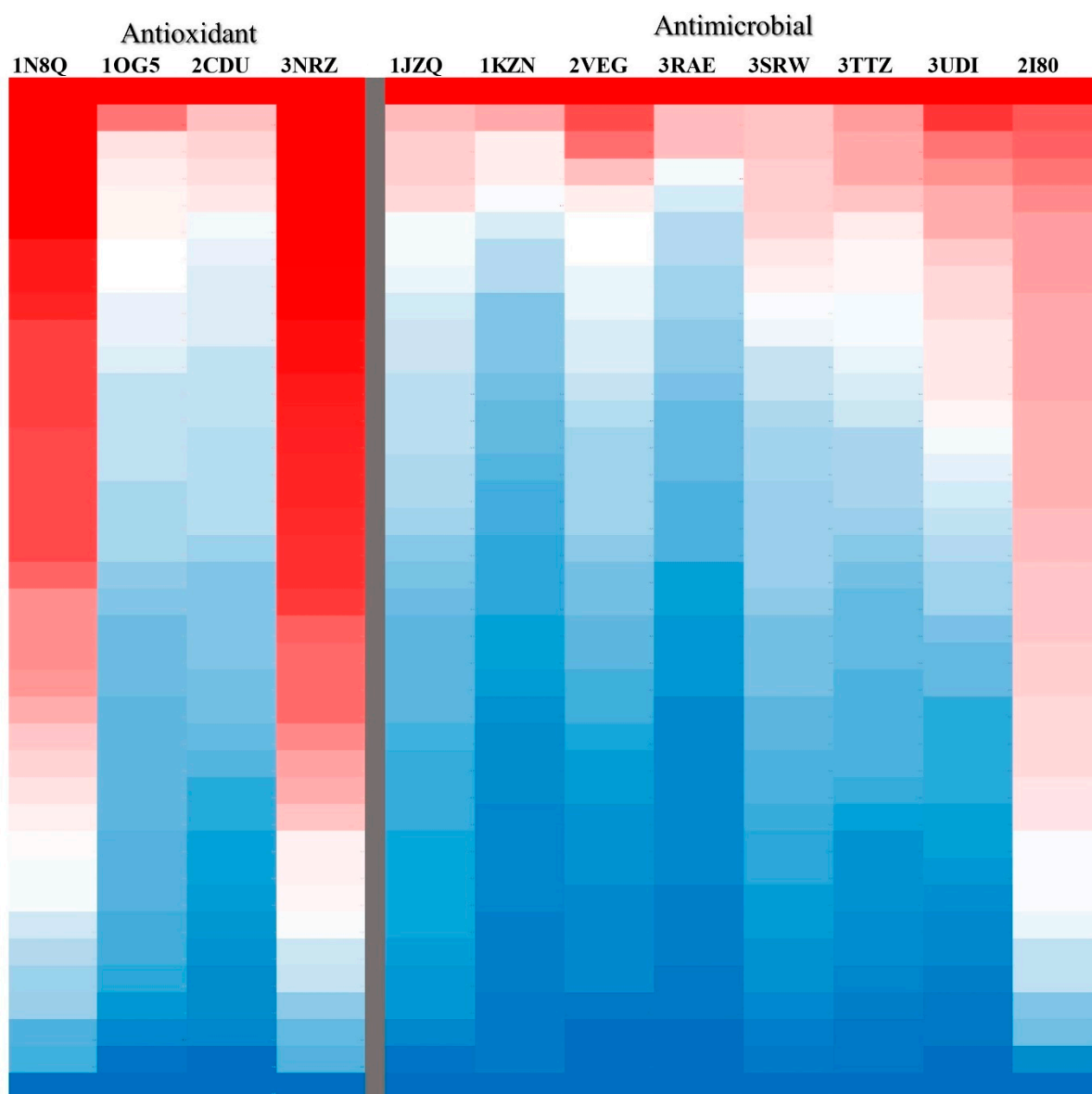


Figure 2. Three-colored heat map (red-white-blue gradient) obtained after coloring each reordered column of the docking scores table in descending order, from red for the ΔG value scored by the native ligand (control), through white for the midpoint interval, and to blue for the highest value (the structure with the lowest affinity).

Compound 29 (4-(3,4-Methylenedioxyphenyl)-2-butanone) was recorded as the highest-scoring structure towards DDI. Binding analysis revealed a good accommodation of the structure in the protein binding pocket (Figure 3). The compound forms four hydrogen bonds (HBs) (Glu16, Leu95, Thr23, and Gly118), two hydrophobic interactions (Phe313, Leu94), and one S-Pi interaction with Met310. This binding pattern is highly similar to that of the native-ligand, which also forms three of the four HB mentioned above (Figure 3).

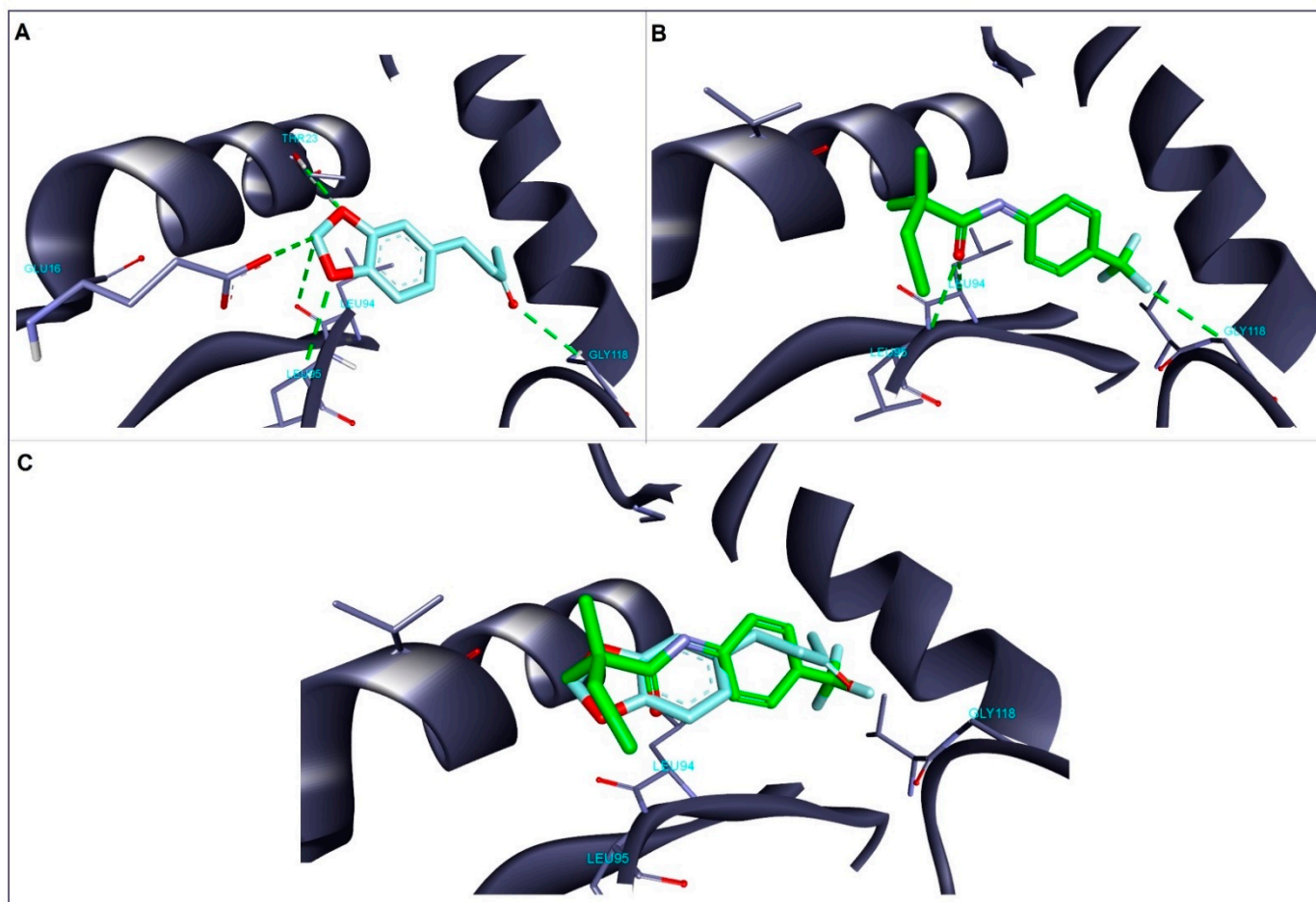


Figure 3. Structure of DDI (2I80) in presence of 4-(3,4-Methylenedioxyphenyl)-2-butanone (29). (A) the native ligand, 3-chloro-2,2-dimethyl-N-[4-(trifluoromethyl)phenyl]propenamide and (B) compound 29 and the native ligand's structures superimposed; (C) HB interactions are depicted as green dotted lines; interacting amino acids are shown as violet sticks.

Terpenes, represent a varied structural group of naturally occurring compounds, with a wide range of pharmacological proprieties. Given their well-documented antioxidant potency, terpenes were shown to induce significant protection against oxidative stress environments in the case of different types of diseases, such as neurodegenerative liver, cardiovascular and renal diseases, cancer, diabetes, and aging [70]. The docking data for the second subset of protein targets, correlated to the antioxidant activity, showed a tendency for the majority of compounds to potentially inhibit xanthine oxidase (3NRZ) and lipoxygenase (1N8Q), the results being very close.

Xanthine oxidase (XO) is the enzyme responsible for the metabolisation of hypoxanthine to xanthine and further to uric acid. The inhibition of XO was shown to reduce vascular oxidative stress and circulating levels uric acid [71]. Docking results show that four of the assessed compounds recorded a superior affinity compared to that of the native ligand, hypoxanthine (−6.7 kcal/mol). These compounds include 4-(3,4-Methylenedioxyphenyl)-2-butanone (29), (2E)-2-Hexenyl benzoate (6), (S)-(+)-Carvone (16), and 2-Bornene, with compound 29 showing the highest calculated affinity for XO. Binding analysis reveals the formation of 3HB (Val1011, Thr1010, Ala1079), two of which are also observed in the case of the native ligand hypoxanthine and several other hydrophobic interactions, which stabilize the molecule in a tight conformation (Figure 4). Previous reports showed that rich monoterpene EOs exerted a significant antioxidant effect, assessed by a HPLC-based assay that quantifies the activity of xanthine oxydase [72].

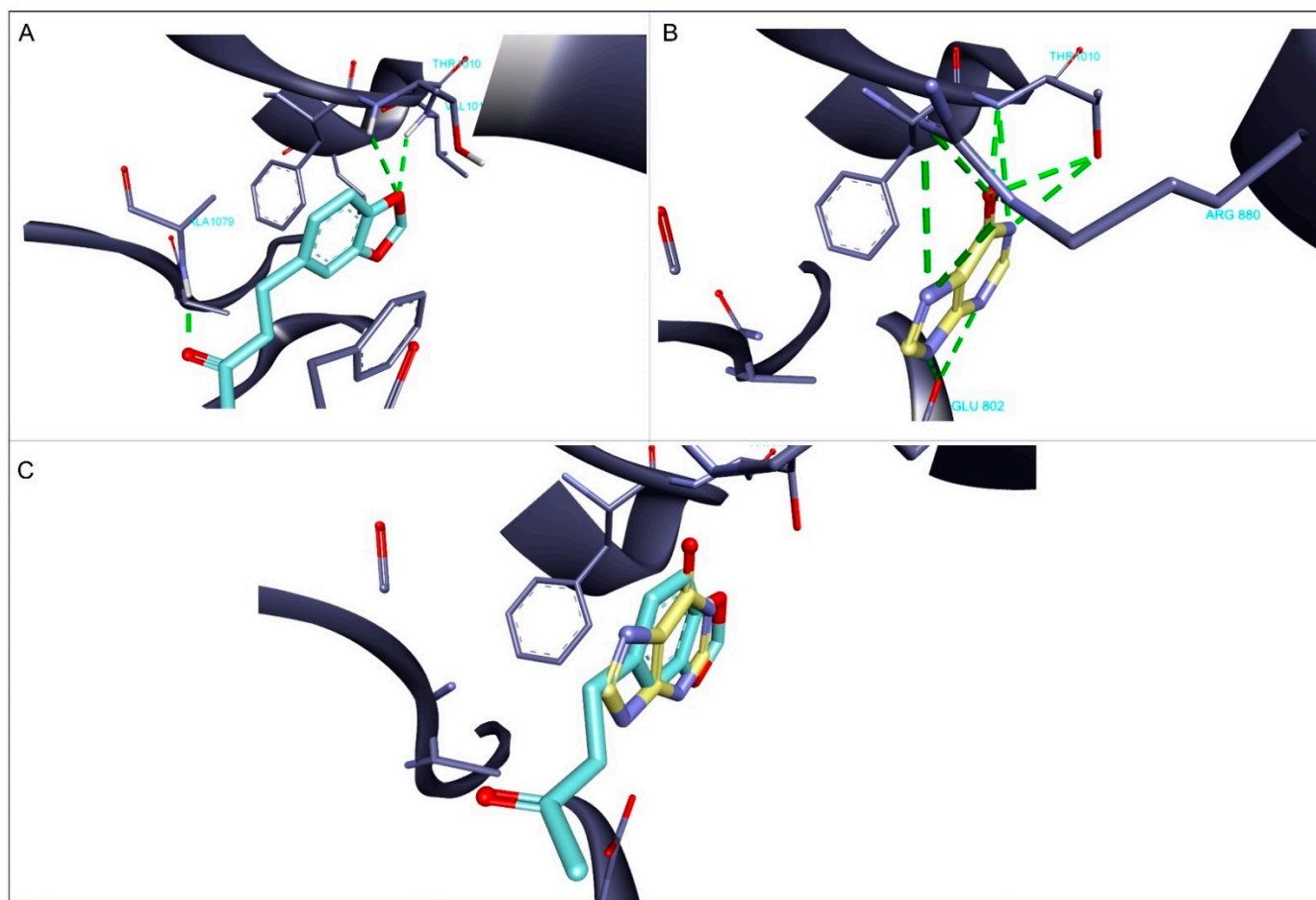


Figure 4. Structure of XO (3NRZ) in complex with 4-(3,4-Methylenedioxyphenyl)-2-butanone (29). (A) the native ligand, hypoxanthine; (B) compound 29 and the native ligand's structures superimposed; and (C) HB interactions are depicted as green dotted lines; interacting amino acids are shown as violet sticks.

In the case of lipoxygenase (LOX) (1N8Q), three compounds scored higher than the native ligand. These structures include the two stereoisomers of 4-Carene (3,12) and p-Cymene (9). The most active compound, 4-Carene interacts with the active site of LOX through multiple hydrophobic interactions, as presented in Figure 5. LOX is, among others, a polyunsaturated fatty acid (PUFA) metabolizing enzyme. PUFA metabolites profoundly affect inflammatory diseases and cancer progression [32]. Therefore, antioxidant compounds that act as LOX inhibitors may reduce these problems. These findings are in line with a previous study that showed the inhibitory LOX activity of terpene-containing orange juice extracts. The study also showed that some extracts elicited LOX inhibitory activity comparable to the known inhibitor quercetin [73].

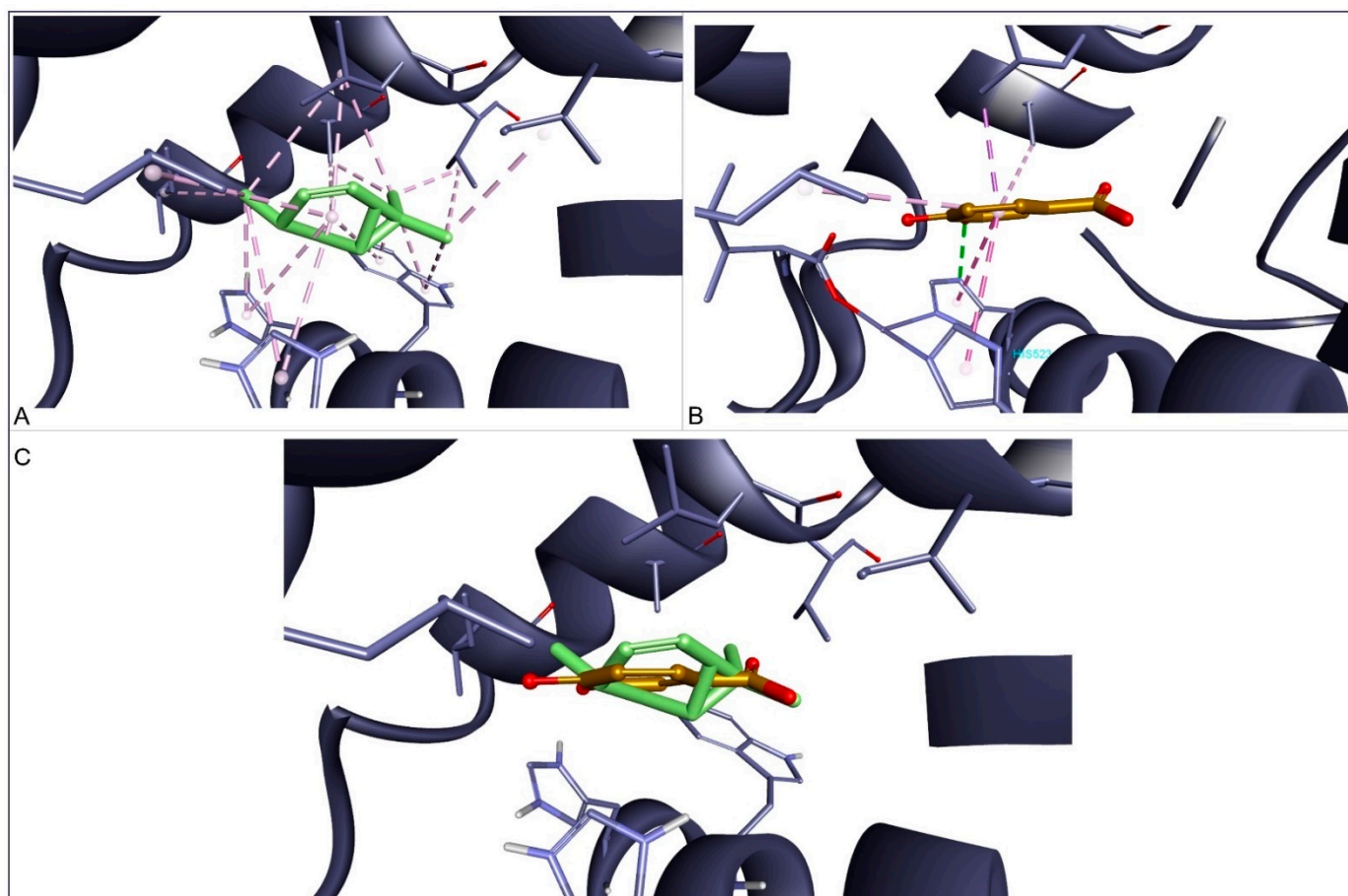


Figure 5. Structure of LOX (1N8Q) in presence of 4-Carene (3). (A) the native ligand, protocatechuic acid; (B) compound 3 and the native ligand's structures superimposed; and (C) hydrophobic interactions are depicted as purple dotted lines and HB as green dotted lines; interacting amino acids are shown as violet sticks.

4. Conclusions

The current research reveals that the volatile oil extracted from the aerial parts of *R. graveolens* L. is rich in ketone compounds, mainly 2-Undecanone and 2-Nonanone. The oil exhibits broad-spectrum antifungal and antibacterial effect along with moderate antioxidants properties revealed by DPPH and β -carotene/linoleic acid bleaching assays. However, the oil inhibited the formation of primary oxidation products is significantly stronger ($p < 0.001$) than BHA between the 8th and 16th days of the incubation period. Furthermore, molecular docking analysis showed that the RGEO could exert its antimicrobial activity by inhibiting the DDI enzyme. The compound with the highest affinity (29) binds in the active site through HB interactions (Glu16, Leu95, Thr23, and Gly118), sharing a high similarity with the native ligand. RGEO compounds may also induce an in vitro antioxidant effect through cumulative XO and LOX inhibition. The highest in silico active compounds showed increased affinity for XO inhibition (compound 29 through HB formation with Val1011, Thr1010, Ala1079) and LOX inhibition (compound 3) mainly through a high number of hydrophobic interactions. Consequently, the analyzed oil could be a new source of natural preservatives and antioxidants in various food and pharmaceutical industry applications.

Author Contributions: Conceptualization and methodology, C.J., C.Ş., and D.S.; investigation, D.M., C.M., G.B., A.T.L.-G., L.-C.R., A.M., M.M., and I.C.; statistical analysis, I.G.; writing—original draft preparation, C.J., D.I.H., and C.M.; writing—review and editing, C.J., D.I.H., and C.M. All authors have read and agreed to the published version of the manuscript.

Funding: This research received no external funding.

Institutional Review Board Statement: Not applicable.

Informed Consent Statement: Not applicable.

Data Availability Statement: The data published in this research are available on request from the first author and corresponding authors.

Acknowledgments: The authors would like to thank the entire team of the Interdisciplinary Research Platform belonging to Banat University of Agricultural Sciences and Veterinary Medicine “King Michael I of Romania” from Timisoara for their support during our study. This paper is published from the own funds of the Banat University of Agricultural Sciences and Veterinary Medicine “King Michael I of Romania” from Timisoara.

Conflicts of Interest: The authors declare no conflict of interest.

References

- Bautista, D.A. Spoilage Problems. Problems Caused by Bacteria. In *Encyclopedia of Food Microbiology*, 2nd ed.; Batt, C.A., Tortorello, M.L., Eds.; Academic Press: Oxford, UK, 2014; pp. 465–470.
- Petruzzi, L.; Corbo, M.R.; Sinigaglia, M.; Bevilacqua, A. Microbial Spoilage of Foods: Fundamentals. In *The Microbiological Quality of Food*; Bevilacqua, A., Corbo, M.R., Sinigaglia, M., Eds.; Woodhead Publishing: Kidlington, UK, 2017; Chapter 1; pp. 1–21.
- Roberta, A.M.; Alejandra, P.G. Quorum Sensing as a Mechanism of Microbial Control and Food Safety. In *Microbial Contamination and Food Degradation*; Holban, A.M., Grumezescu, A.M., Eds.; Academic Press: London, UK, 2018; Chapter 4; pp. 85–107.
- Gustavsson, J.; Cederberg, C.; Sonesson, U. *Global Food Losses and Food Waste*; Swedish Institute for Food and Biotechnology SIK: Gothenburg, Sweden, 2011.
- Hossain, A.; Shah, M.D.; Sang, S.V.; Sakari, M. Chemical composition and antibacterial properties of the essential oils and crude extracts of *Merremia borneensis*. *J. King Saud Univ. Sci.* **2012**, *24*, 243–249. [[CrossRef](#)]
- Orlanda, J.F.F.; Nascimento, A. Chemical composition and antibacterial activity of *Ruta graveolens* L. (Rutaceae) volatile oils, from São Luís, Maranhão, Brazil. *S. Afr. J. Bot.* **2015**, *99*, 103–106. [[CrossRef](#)]
- Xu, X.; Liu, A.; Hu, S.; Ares, I.; Martínez-Larrañaga, M.-R.; Wang, X.; Martínez, M.; Anadón, A.; Martínez, M.-A. Synthetic phenolic antioxidants: Metabolism, hazards and mechanism of action. *Food Chem.* **2021**, *353*, 129488. [[CrossRef](#)]
- Sahu, S.C.; Green, S. Food Antioxidants: Their Dual Role in Carcinogenesis. In *Oxidants, Antioxidants, and Free Radicals*; CRC Press: Boca Raton, FL, USA, 2017; pp. 327–340.
- Álvarez-Martínez, F.; Barrañón-Catalán, E.; Herranz-López, M.; Micol, V. Antibacterial plant compounds, extracts and essential oils: An updated review on their effects and putative mechanisms of action. *Phytomedicine* **2021**, *90*, 153626. [[CrossRef](#)] [[PubMed](#)]
- Alves, M.J.; Froufe, H.J.; Costa, A.F.; Santos, A.F.; Oliveira, L.G.; Osório, S.R.; Abreu, R.; Pintado, M.; Ferreira, I.C. Docking studies in target proteins involved in antibacterial action mechanisms: Extending the knowledge on standard antibiotics to antimicrobial mushroom compounds. *Molecules* **2014**, *19*, 1672–1684. [[CrossRef](#)] [[PubMed](#)]
- Wei, L.; Wang, Y.Z.; Li, Z.Y. Floral ontogeny of Ruteae (Rutaceae) and its systematic implications. *Plant Biol.* **2012**, *14*, 190–197. [[CrossRef](#)]
- Wei, L.; Xiang, X.-G.; Wang, Y.-Z.; Li, Z.-Y. Phylogenetic relationships and evolution of the androecia in Ruteae (Rutaceae). *PLoS ONE* **2015**, *10*, e0137190. [[CrossRef](#)]
- Coimbra, A.T.; Ferreira, S.; Duarte, A.P. Genus *Ruta*: A natural source of high value products with biological and pharmacological properties. *J. Ethnopharmacol.* **2020**, *260*, 113076. [[CrossRef](#)]
- Attia, E.Z.; Abd El-Baky, R.M.; Desoukey, S.Y.; El Hakeem Mohamed, M.A.; Bishr, M.M.; Kamel, M.S. Chemical composition and antimicrobial activities of essential oils of *Ruta graveolens* plants treated with salicylic acid under drought stress conditions. *Future J. Pharm. Sci.* **2018**, *4*, 254–264. [[CrossRef](#)]
- Alexan, M.; Bojor, O.; Craciun, F. *The Drug Flora in Romania*; Ceres Publishing House: Bucharest, Romania, 1991; pp. 161–162. (In Romanian)
- Stashenko, E.E.; Acosta, R.; Martínez, J.R. High-resolution gas-chromatographic analysis of the secondary metabolites obtained by subcritical-fluid extraction from Colombian rue (*Ruta graveolens* L.). *J. Biochem. Biophys. Methods* **2000**, *43*, 379–390. [[CrossRef](#)]
- De Feo, V.; De Simone, F.; Senatore, F. Potential allelochemicals from the essential oil of *Ruta graveolens*. *Phytochemistry* **2002**, *61*, 573–578. [[CrossRef](#)]
- Mejri, J.; Abderrabba, M.; Mejri, M. Chemical composition of the essential oil of *Ruta chalepensis* L.: Influence of drying, hydro-distillation duration and plant parts. *Ind. Crop. Prod.* **2010**, *32*, 671–673. [[CrossRef](#)]
- Ahmad, N.; Faisal, M.; Anis, M.; Aref, I. In vitro callus induction and plant regeneration from leaf explants of *Ruta graveolens* L. *S. Afr. J. Bot.* **2010**, *76*, 597–600. [[CrossRef](#)]
- Muntean, D.; Licker, M.; Alexa, E.; Popescu, I.; Jianu, C.; Buda, V.; Dehelean, C.A.; Ghiulai, R.; Horhat, F.; Horhat, D.; et al. Evaluation of essential oil obtained from *Mentha × piperita* L. against multidrug-resistant strains. *Infect. Drug Resist.* **2019**, *12*, 2905–2914. [[CrossRef](#)] [[PubMed](#)]

21. Adams, R.P. *Identification of essential oil components by gas chromatography/mass spectrometry*, 4th ed.; Allured Publishing Corporation: Carol Stream, IL, USA, 2007.
22. ISO. *Animal and Vegetable Fats and Oils-Determination of Peroxide Value-Potentiometric End-Point Determination*; ISO 27107:2010; International Organization for Standardization: Geneva, Switzerland, 2010.
23. Jianu, C.; Goleț, I.; Stoin, D.; Cocan, I.; Lukinich-Gruia, A.T. Antioxidant activity of *Pastinaca sativa* L. ssp. *sylvestris* [Mill.] Rouy and Camus Essential Oil. *Molecules* **2020**, *25*, 869. [[CrossRef](#)]
24. Jianu, C.; Mișcă, C.; Muntean, S.G.; Lukinich-Gruia, A.T. Composition, antioxidant and antimicrobial activity of the essential oil of *Achillea collina* Becker growing wild in Western Romania. *Hem. Ind.* **2015**, *69*, 381–386. [[CrossRef](#)]
25. Rodriguez-Tudela, J.L.; Arendrup, M.C.; Barchiesi, F.; Bille, J.; Chryssanthou, E.; Cuenca-Estrella, M.; Dannaoui, E.; Denning, D.W.; Donnelly, J.P.; Dromer, F.; et al. EUCAST Definitive Document EDef 7.1: Method for the determination of broth dilution MICs of antifungal agents for fermentative yeasts: Subcommittee on Antifungal Susceptibility Testing (AFST) of the ESCMID European Committee for Antimicrobial Susceptibility Testing (EUCAST). *Clin. Microbiol. Infect.* **2008**, *14*, 398–405.
26. Jianu, C.; Moleriu, R.; Stoin, D.; Cocan, I.; Bujancă, G.; Pop, G.; Lukinich-Gruia, A.T.; Muntean, D.; Rusu, L.-C.; Horhat, D.I. Antioxidant and Antibacterial Activity of *Nepeta × faassenii* Bergmans ex Stearn Essential Oil. *Appl. Sci.* **2021**, *11*, 442. [[CrossRef](#)]
27. Jianu, C.; Stoin, D.; Cocan, I.; David, I.; Pop, G.; Lukinich-Gruia, A.T.; Mioc, M.; Mioc, A.; Șoica, C.; Muntean, D. In silico and in vitro evaluation of the antimicrobial and antioxidant potential of *Mentha × smithiana* R. GRAHAM Essential Oil from Western Romania. *Foods* **2021**, *10*, 815. [[CrossRef](#)] [[PubMed](#)]
28. Berman, H.M.; Westbrook, J.; Feng, Z.; Gilliland, G.; Bhat, T.N.; Weissig, H.; Shindyalov, I.N.; Bourne, P.E. The protein data bank. *Nucleic Acids Res.* **2000**, *28*, 235–242. [[CrossRef](#)]
29. Trott, O.; Olson, A.J. AutoDock Vina: Improving the speed and accuracy of docking with a new scoring function, efficient optimization, and multithreading. *J. Comput. Chem.* **2010**, *31*, 455–461. [[CrossRef](#)] [[PubMed](#)]
30. Nakama, T.; Nureki, O.; Yokoyama, S. Structural basis for the recognition of isoleucyl-adenylate and an antibiotic, mupirocin, by isoleucyl-tRNA synthetase. *J. Biol. Chem.* **2001**, *276*, 47387–47393. [[CrossRef](#)] [[PubMed](#)]
31. Lafitte, D.; Lamour, V.; Tsvetkov, P.O.; Makarov, A.A.; Klich, M.; Deprez, P.; Moras, D.; Briand, A.C.; Gilli, R. DNA gyrase interaction with coumarin-based inhibitors: The role of the hydroxybenzoate isopentenyl moiety and the 5'-methyl group of the noviose. *Biochemistry* **2002**, *41*, 7217–7223. [[CrossRef](#)]
32. Borbulevych, O.Y.; Jankun, J.; Selman, S.H.; Skrzypczak-Jankun, E. Lipoygenase interactions with natural flavonoid, quercetin, reveal a complex with protocatechuic acid in its X-ray structure at 2.1 Å resolution. *Proteins Struct. Funct. Bioinform.* **2004**, *54*, 13–19. [[CrossRef](#)]
33. Williams, P.A.; Cosme, J.; Ward, A.; Angove, H.C.; Vinković, D.M.; Jhoti, H. Crystal structure of human cytochrome P450 2C9 with bound warfarin. *Nature* **2003**, *424*, 464–468. [[CrossRef](#)]
34. Lountos, G.T.; Jiang, R.; Wellborn, W.B.; Thaler, T.L.; Bommarius, A.S.; Orville, A.M. The crystal structure of NAD(P)H oxidase from *Lactobacillus sanfranciscensis*: Insights into the Conversion of O₂ into Two Water Molecules by the Flavoenzyme. *Biochemistry* **2006**, *45*, 9648–9659. [[CrossRef](#)]
35. Liu, S.; Chang, J.S.; Herberg, J.T.; Horng, M.-M.; Tomich, P.K.; Lin, A.H.; Marotti, K.R. Allosteric inhibition of Staphylococcus aureus-d-alanine: D-alanine ligase revealed by crystallographic studies. *Proc. Nat. Acad. Sci. USA* **2006**, *103*, 15178–15183. [[CrossRef](#)]
36. Levy, C.; Minnis, D.; Derrick, J.P. Dihydropteroate synthase from Streptococcus pneumoniae: Structure, ligand recognition and mechanism of sulfonamide resistance. *Biochem. J.* **2008**, *412*, 379–388. [[CrossRef](#)]
37. Cao, H.; Pauff, J.M.; Hille, R. Substrate orientation and catalytic specificity in the action of xanthine oxidase: The sequential hydroxylation of hypoxanthine to uric acid. *J. Biol. Chem.* **2010**, *285*, 28044–28053. [[CrossRef](#)] [[PubMed](#)]
38. Veselkov, D.A.; Laponogov, I.; Pan, X.-S.; Selvarajah, J.; Skamrova, G.B.; Branstrom, A.; Narasimhan, J.; Prasad, J.V.V.; Fisher, L.M.; Sanderson, M.R. Structure of a quinolone-stabilized cleavage complex of topoisomerase IV from Klebsiella pneumoniae and comparison with a related Streptococcus pneumoniae complex. *Acta Crystallogr. Sect. D Struct. Biol.* **2016**, *72*, 488–496. [[CrossRef](#)] [[PubMed](#)]
39. Li, X.; Hilgers, M.; Cunningham, M.; Chen, Z.; Trzoss, M.; Zhang, J.; Kohonen, L.; Lam, T.; Creighton, C.; Kedar, G.; et al. Structure-based design of new DHFR-based antibacterial agents: 7-aryl-2,4-diaminoquinazolines. *Bioorganic Med. Chem. Lett.* **2011**, *21*, 5171–5176. [[CrossRef](#)]
40. Sherer, B.A.; Hull, K.; Green, O.; Basarab, G.; Hauck, S.; Hill, P.; Loch, J.T., III; Mullen, G.; Bist, S.; Bryant, J. Pyrrolamide DNA gyrase inhibitors: Optimization of antibacterial activity and efficacy. *Bioorgan. Med. Chem. Lett.* **2011**, *21*, 7416–7420. [[CrossRef](#)]
41. Han, S.; Caspers, N.; Zaniewski, R.P.; Lacey, B.M.; Tomaras, A.P.; Feng, X.; Geoghegan, K.F.; Shanmugasundaram, V. Distinctive Attributes of β-Lactam Target Proteins in Acinetobacter baumannii Relevant to Development of New Antibiotics. *J. Am. Chem. Soc.* **2011**, *133*, 20536–20545. [[CrossRef](#)] [[PubMed](#)]
42. De Pooter, H.L.; Nicolai, B.; De Laet, J.; De Buyck, L.F.; Schamp, N.M.; Goetghebeur, P. The essential oils of five *Nepeta* Species. A preliminary evaluation of their use in chemotaxonomy by cluster analysis. *Flavour Fragr. J.* **1988**, *3*, 155–159. [[CrossRef](#)]
43. Radulovic, N.; Blagojevic, P.D.; Rabbitt, K.; de Sousa Menezes, F. Essential oil of *Nepeta × faassenii* Bergmans ex Stearn (*N. mussinii* Spreng. × *N. nepetella* L.): A comparison study. *Nat. Prod. Commun.* **2011**, *6*, 1015–1022. [[CrossRef](#)]
44. Yaacob, K.B.; Abdullah, C.M.; Joulain, D. Essential Oil of *Ruta graveolens* L. *J. Essent. Oil Res.* **1989**, *1*, 203–207. [[CrossRef](#)]

45. Haddouchi, F.; Chaouche, T.M.; Zaouali, Y.; Ksouri, R.; Attou, A.; Benmansour, A. Chemical composition and antimicrobial activity of the essential oils from four *Ruta* species growing in Algeria. *Food Chem.* **2013**, *141*, 253–258. [[CrossRef](#)] [[PubMed](#)]
46. Formisano, C.; Delfino, S.; Oliviero, F.; Tenore, G.C.; Rigano, D.; Senatore, F. Correlation among environmental factors, chemical composition and antioxidative properties of essential oil and extracts of chamomile (*Matricaria chamomilla* L.) collected in Molise (South-central Italy). *Ind. Crop. Prod.* **2015**, *63*, 256–263. [[CrossRef](#)]
47. El-Sherbeny, S.; Hussein, M.; Khalil, M. Improving the production of *Ruta graveolens* L. plants cultivated under different compost levels and various sowing distance. *Am.-Euras. J. Agric. Environ. Sci.* **2007**, *23*, 271–281.
48. Soleimani, M.; Azar, P.A.; Saber-Tehrani, M.; Rustaiyan, A. Volatile composition of *Ruta graveolens* L. of North of Iran. *World Appl. Sci. J.* **2009**, *7*, 124–126.
49. Reddy, D.N.; Al-Rajab, A.J. Chemical composition, antibacterial and antifungal activities of *Ruta graveolens* L. volatile oils. *Cogent Chem.* **2016**, *2*, 1220055. [[CrossRef](#)]
50. Narimani, R.; Moghaddam, M.; Ghasemi Pirbalouti, A.; Mojarab, S. Essential oil composition of seven populations belonging to two *Nepeta* species from Northwestern Iran. *Int. J. Food Prop.* **2017**, *20* (Suppl. S2), 2272–2279.
51. Li, T.; Hu, W.; Li, J.; Zhang, X.; Zhu, J.; Li, X. Coating effects of tea polyphenol and rosemary extract combined with chitosan on the storage quality of large yellow croaker (*Pseudosciaena crocea*). *Food Control* **2012**, *25*, 101–106. [[CrossRef](#)]
52. Singh, G.; Kapoor, I.; Singh, P.; de Heluani, C.S.; de Lampasona, M.P.; Catalan, C.A.N. Chemistry, antioxidant and antimicrobial investigations on essential oil and oleoresins of *Zingiber officinale*. *Food Chem. Toxicol.* **2008**, *46*, 3295–3302. [[CrossRef](#)]
53. Benali, T.; Habbadi, K.; Khabbach, A.; Marmouzi, I.; Zengin, G.; Bouyahya, A.; Chamkhi, I.; Chtibi, H.; Aanniz, T.; Achbani, E.H.; et al. GC–MS analysis, antioxidant and antimicrobial activities of *Achillea Odorata* Subsp. *Pectinata* and *Ruta Montana* essential oils and their potential use as food preservatives. *Foods* **2020**, *9*, 668. [[CrossRef](#)]
54. Mohammedi, H.; Mecherara-Idjeri, S.; Hassani, A. Variability in essential oil composition, antioxidant and antimicrobial activities of *Ruta montana* L. collected from different geographical regions in Algeria. *J. Essent. Oil Res.* **2019**, *32*, 88–101. [[CrossRef](#)]
55. Jaradat, N.; Adwan, L.; K’Aibni, S.; Zaid, A.N.; Shtaya, M.; Shraim, N.; Assali, M. Variability of Chemical Compositions and Antimicrobial and Antioxidant Activities of *Ruta chalepensis* Leaf Essential Oils from Three Palestinian Regions. *BioMed Res. Int.* **2017**, *2017*, 2672689. [[CrossRef](#)]
56. Althaher, A.R.; Oran, S.A.; Bustanji, Y.K. Phytochemical analysis, in vitro assessment of antioxidant properties and cytotoxic potential of *Ruta chalepensis* L. essential oil. *J. Essent. Oil Bear. Plants* **2020**, *23*, 1409–1421. [[CrossRef](#)]
57. Oke, F.; Aslim, B.; Ozturk, S.; Altundag, S. Essential oil composition, antimicrobial and antioxidant activities of *Satureja cuneifolia* Ten. *Food Chem.* **2009**, *112*, 874–879. [[CrossRef](#)]
58. Kulisic, T.; Radonic, A.; Katalinic, V.; Milos, M. Use of different methods for testing antioxidative activity of oregano essential oil. *Food Chem.* **2004**, *85*, 633–640. [[CrossRef](#)]
59. Loizzo, M.; Falco, T.; Bonesi, M.; Sicari, V.; Tundis, R.; Bruno, M. *Ruta chalepensis* L. (Rutaceae) leaf extract: Chemical composition, antioxidant and hypoglycaemic activities. *Nat. Prod. Res.* **2018**, *32*, 521–528. [[CrossRef](#)]
60. Aligiannis, N.; Kalpoutzakis, E.; Mitaku, S.; Chinou, I.B. Composition and antimicrobial activity of the essential oils of two *Origanum* species. *J. Agric. Food Chem.* **2001**, *49*, 4168–4170. [[CrossRef](#)]
61. Angienda, P.O.; Onyango, D.M.; Hill, D.J. Potential application of plant essential oils at sub-lethal concentrations under extrinsic conditions that enhance their antimicrobial effectiveness against pathogenic bacteria. *Afr. J. Microbiol. Res.* **2010**, *4*, 1678–1684.
62. Gilles, M.; Zhao, J.; An, M.; Agboola, S. Chemical composition and antimicrobial properties of essential oils of three Australian *Eucalyptus* species. *Food Chem.* **2010**, *119*, 731–737. [[CrossRef](#)]
63. Cox, S.; Mann, C.; Markham, J.; Bell, H.C.; Gustafson, J.; Warmingington, J.; Wyllie, S.G. The mode of antimicrobial action of the essential oil of *Melaleuca alternifolia* (tea tree oil). *J. Appl. Microbiol.* **2000**, *88*, 170–175. [[CrossRef](#)] [[PubMed](#)]
64. Franchini, S.; Prandi, A.; Baraldi, A.; Sorbi, C.; Tait, A.; Buccioni, M.; Marucci, G.; Cilia, A.; Pirona, L.; Fossa, P. 1,3-Dioxolane-based ligands incorporating a lactam or imide moiety: Structure–affinity/activity relationship at α 1-adrenoceptor subtypes and at 5-HT_{1A} receptors. *Eur. J. Med. Chem.* **2010**, *45*, 3740–3751. [[CrossRef](#)]
65. Fossa, P.; Cichero, E. In silico evaluation of human small heat shock protein HSP27: Homology modeling, mutation analyses and docking studies. *Bioorgan. Med. Chem.* **2015**, *23*, 3215–3220. [[CrossRef](#)] [[PubMed](#)]
66. Tonelli, M.; Espinoza, S.; Gainetdinov, R.; Cichero, E. Novel biguanide-based derivatives scouted as TAAR1 agonists: Synthesis, biological evaluation, ADME prediction and molecular docking studies. *Eur. J. Med. Chem.* **2017**, *127*, 781–792. [[CrossRef](#)]
67. Goncharov, N.V.; Avdonin, P.V.; Nadeev, A.D.; Zharkikh, I.L.; Jenkins, R.O. Reactive oxygen species in pathogenesis of atherosclerosis. *Curr. Pharm. Des.* **2015**, *21*, 1134–1146. [[CrossRef](#)]
68. Trombetta, D.; Castelli, F.; Sarpietro, M.G.; Venuti, V.; Cristani, M.; Daniele, C.; Saija, A.; Mazzanti, G.; Bisignano, G. Mechanisms of antibacterial action of three monoterpenes. *Antimicrob. Agents Chemother.* **2005**, *49*, 2474–2478. [[CrossRef](#)] [[PubMed](#)]
69. Zengin, H.; Baysal, A.H. Antibacterial and Antioxidant activity of essential oil terpenes against pathogenic and spoilage-forming bacteria and cell structure-activity relationships evaluated by SEM microscopy. *Molecules* **2014**, *19*, 17773–17798. [[CrossRef](#)] [[PubMed](#)]
70. Gonzalez-Burgos, E.; Gómez-Serranillos, M. Terpene compounds in nature: A review of their potential antioxidant activity. *Curr. Med. Chem.* **2012**, *19*, 5319–5341. [[CrossRef](#)]
71. Kostić, D.A.; Dimitrijević, D.S.; Stojanović, G.; Palić, I.R.; Đorđević, A.; Ickovski, J. Xanthine oxidase: Isolation, assays of activity, and inhibition. *J. Chem.* **2015**, *2015*, 294858. [[CrossRef](#)]

-
72. Salles Trevisan, M.T.; Vasconcelos Silva, M.G.; Pfundstein, B.; Spiegelhalter, B.; Owen, R.W. Characterization of the volatile pattern and antioxidant capacity of essential oils from different species of the genus *Ocimum*. *J. Agric. Food Chem.* **2006**, *54*, 4378–4382. [[CrossRef](#)] [[PubMed](#)]
 73. Sánchez-Martínez, J.D.; Bueno, M.; Alvarez-Rivera, G.; Tudela, J.; Ibañez, E.; Cifuentes, A. In vitro neuroprotective potential of terpenes from industrial orange juice by-products. *Food Funct.* **2021**, *12*, 302–314. [[CrossRef](#)]